Density gradients to reduce fluid instabilities in multishell inertial-confinement-fusion targets

K. O. Mikaelian and J. D. Lindl
Lawrence Livermore National Laboratory, University of California, Livermore, California 94550
(Received 9 May 1983)

The growth of Rayleigh-Taylor instabilities in inertial-confinement-fusion targets can be reduced if smooth density gradients are introduced at the interfaces. Keeping the total mass fixed, we consider spreading a heavy shell either continuously or in a discrete number of subshells. We calculate the rate for the fastest growing mode as a function of the fraction of mass spread and find the minima for the cases of 4, 6, and 8 subshells. The rates are reduced by 1.4—1.6. If all the mass is spread continuously into an exponential profile, we find that the rates are reduced by approximately $\sqrt{2\pi}\approx 2.5$.

I. INTRODUCTION

Fluid instabilities are a well-known source of failure for the implosion of inertial-confinement-fusion (ICF) targets. Rayleigh-Taylor instabilities are particularly a problem in designs calling for multiple shells when, sometime during the history of implosion, one finds a shell of light material (density $\rho_l \sim 1$ g/cm^3) accelerating a shell of heavy material (density $\rho_h \sim 20$ g/cm^3). While much work[1–5] has gone in studying the stability of the outermost shell during ablation (laser pulse shaping,[2] ablative stabilization,[1,3] thermal conduction,[4] and, more recently, the effect of the Kelvin-Helmholtz instability[5]), little work has been done on the inner shells.

One possibility[6] to reduce the growth of Rayleigh-Taylor instabilities is to introduce an energy spread in the driver. Effectively this approach spreads the region where energy is absorbed and benefits from the stabilizing effect of a density gradient.[7] In this paper we explore the advantages of density gradients directly by giving some structure to one or more of the shells (Fig. 1), a technique that can be applied to both single-shell and multishell targets.

Classically[8] small density perturbations at the interface between two shells grow exponentially with time, $e^{\gamma t}$, with the rate γ given by

$$\gamma_{\text{classical}}=[gk(\rho_h-\rho_l)/(\rho_h+\rho_l)]^{1/2}\,, \tag{1}$$

where g is the acceleration (assumed constant) and $k=2\pi/\lambda$, λ is the wavelength of density perturbations. Equation (1) is valid if λ is much less than the thickness of each shell. Typically $g\sim 5\times 10^{15}$ to 5×10^{16} cm/s^2, and Eq. (1) leads to an unacceptably large number of e-foldings. We expect smaller rates by smoothing the sharp transition from ρ_l to ρ_h. This approach might be described as reducing the Atwood number $(\rho_h-\rho_l)/(\rho_h+\rho_l)$ to a smaller "effective" Atwood number to reduce γ.

Since heavy shells are usually thin one might worry about the effect of finite thickness of ρ_h. For a shell of thickness t_0, Eq. (1) is replaced by

$$\gamma=\{gk(\rho_h-\rho_l)/[\rho_h+\rho_l\coth(kt_0)]\}^{1/2} \tag{2}$$

and the effect is negligible since, as we argue later, $kt_0=2\pi t_0/\lambda\sim 2\pi$. In addition to this unstable mode for finite thickness shells there is a stable oscillatory mode with $\gamma=i\sqrt{gk}$.

Many other modes appear when the interface is given some structure as in Fig. 1. There are infinitely many modes if the structure is continuous, and $n+2$ modes if the structure consists of n discrete subshells. In this paper we describe the calculation of the growth rates and how to

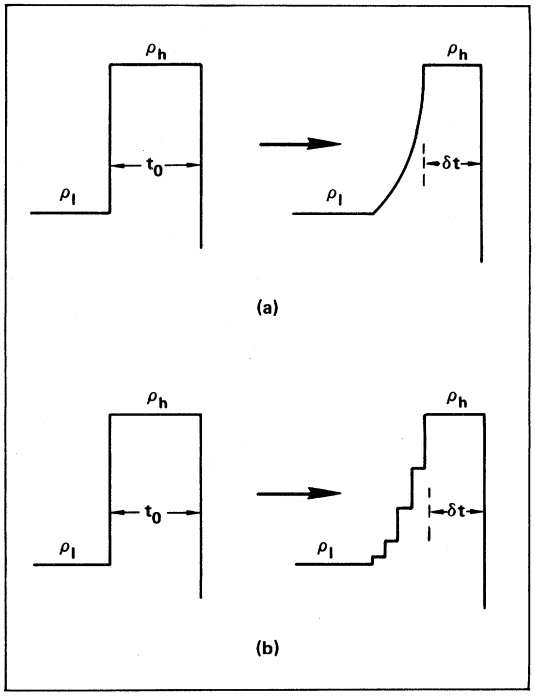

FIG. 1. Shell of high density ρ_h and of original thickness t_0 is partially spread into (a) a continuous profile or (b) a discrete number of subshells. The remaining shell of density ρ_h has thickness δt.

reduce the fastest growing mode by spreading a certain fraction of the original mass, i.e., $\rho_h t_0$, into a number of subshells. Since the hydrodynamic efficiency in an implosion depends on this mass, all our calculations take a fixed (but otherwise arbitrary) amount of mass and spread it, continuously or stepwise, into subshells.

In Sec. II we describe briefly the general formalism[8] used to obtain the growth rates. In Sec. III we apply that formalism to a continuous density gradient [Fig. 1(a)] and in Sec. IV we consider discrete density jumps [Fig. 1(b)]. Finally, in Sec. V we give our results by plotting the fastest growth rate $\gamma^{\max}$ versus fraction of mass spread into subshells (Fig. 4). In all our numerical examples $\rho_l = 1$ g/cm^3 and $\rho_h = 20$ g/cm^3, $t_0 = 1$ for scale.

II. GENERAL FORMALISM

The growth rates are found by solving the differential equation[8] ($D \equiv d/dy$)

$$D(\rho DW) + \frac{gk^2}{\gamma^2} WD\rho - k^2 \rho W = 0 , \tag{3}$$

where the density $\rho(y)$ is assumed to vary only in the y direction, with perturbations $\delta\rho = \delta\rho(y) e^{ikx+\gamma t}$, and $W(y)$ is the y-dependent part of the perturbed fluid velocity. Equation (3) is obtained by linearizing the hydrodynamic equations assuming $\delta\rho \ll \rho$, and assuming incompressible fluids. Surface tension, viscosity, and heat transfer are neglected in this equation, in which γ^2/g must be viewed as an eigenvalue and $W^\gamma(y)$ as the eigenfunction.

Integrating Eq. (3) across a thin interface we obtain

$$\Delta\left[\rho \frac{dW}{dy}\right] + \frac{gk^2}{\gamma^2} W\Delta(\rho) = 0 , \tag{4}$$

where $\Delta(f) = f_+ - f_-$ with $f_\pm$ equal to the value of f above (below) the boundary. W is continuous everywhere, but, since we are neglecting viscosity, dW/dy need not be continuous. Equation (4) is a condition to be satisfied by W at the boundaries or interfaces (note that it contains the eigenvalue γ one is trying to determine).

The condition at a free boundary can be gotten from Eq. (4) by setting ρ_+ or $\rho_- = 0$, and it reads $dW/dy + (gk^2/\gamma^2)W = 0$, where W and dW/dy are evaluated at the free boundary. At a boundary where the density, but not necessarily its derivative is continuous as in Fig. 1(a), then Eq. (4) implies that dW/dy is also continuous.

The condition at a fixed boundary reads $W = 0$. If one of the shells, e.g., ρ_l, is very thick compared to the wavelength λ of perturbations, then $W \sim e^{-k|y|}$ and vanishes only at "infinity." We have used this condition on W in the region $\rho = \rho_l$, though our codes can handle a finite thickness low-density shell. The difference is negligible if λ is less than the thickness of ρ_l, a condition well satisfied in our applications. Of course, the thickness of the *heavy* shell t_0 is finite and in fact is used as scale for length.

III. CONTINUOUS DENSITY PROFILE

If the mass $\rho_h t_0$ of the original heavy shell is spread continuously as in Fig. 1(a), then in addition to the one stable mode $\gamma^2 = -gk$ there will be an infinite number of unstable modes which we proceed to calculate. In practice one is usually interested in the first two or three fastest growing modes.

The calculation of the eigenmodes for continuous density profiles is quite complicated because one must solve the differential equation Eq. (3) for arbitrary k and γ and then find the admissible values of γ by matching to the proper boundary conditions. Only the cases $\rho = \text{const}$ and $\rho = \rho_0 e^{\beta y}$ can be solved analytically with a reasonable amount of effort, and in this section we consider the following density profile:

$$\rho = \begin{cases} \rho_l, & y \le 0 \\ \rho_l e^{\beta y}, & 0 \le y \le t \\ \rho_h = \rho_l e^{\beta t}, & t \le y \le t + \delta t \\ 0, & t + \delta t < y . \end{cases} \tag{5}$$

Fortunately, the exponential density profile not only can be solved exactly but it turns out to be the best density profile to reduce the fastest growing mode.[9] One could improve on the density profile given above by introducing density jumps on the two sides of the exponential. The jumps are wavelength dependent and vanish as $\lambda \to 0$. For wavelengths several times the thickness of the shell (or shorter) the effect of the jumps is less than a few percent, which we neglected and instead chose a density profile continuous at $y = 0$ and at $y = t$. The thickness of the remanining heavy shell is δt. Both t and δt are arbitrary, and a free boundary at $y = t + \delta t$ is denoted by $\rho = 0$ as mentioned earlier.

In regions of constant density like $y \le 0$ and $t \le y \le t + \delta t$, the differential equation (3) reduces to $(D^2 - k^2)W(y) = 0$, hence $W \sim e^{\pm ky}$. In the region $0 \le y \le t$, substituting $\rho = \rho_l e^{\beta y}$ in Eq. (3) gives

$$D^2 W + \beta DW - k^2 \left[1 - \frac{g\beta}{\gamma^2}\right] W = 0 \tag{6}$$

whose general solution is $W = A_1 e^{q_1 y} + A_2 e^{q_2 y}$ where A_1 and A_2 are constants and $q_{1,2}$ are solutions to the quadratic equation

$$q^2 + q\beta - k^2 \left[1 - \frac{g\beta}{\gamma^2}\right] = 0 . \tag{7}$$

The two roots satisfy $q_1 + q_2 = -\beta$. It will prove useful to define the dimensionless quantities

$$\begin{aligned} e &= kt , \\ d &= \beta t/2 , \\ x &= (q_1 - q_2)t/2i , \end{aligned} \tag{8}$$

in terms of which

$$\frac{\gamma^2}{gk} = \frac{2ed}{x^2 + d^2 + e^2} . \tag{9}$$

For given k, t, and β the growth rates $\gamma/\sqrt{g}$ are determined from Eq. (9) once we know x, which is found by requiring that the eigenfunction(s) W satisfy the proper

boundary conditions. Corresponding to Eq. (5) we have

$$W=\begin{cases} Ae^{ky}, & y\le 0 \\ A_1e^{q_1y}+A_2e^{q_2y}, & 0\le y\le t \\ B_1e^{ky}+B_2e^{-ky}, & t\le y\le t+\delta t. \end{cases} \tag{10}$$

There are five boundary conditions: continuity of W at $y=0$ requires

$$A=A_1+A_2\ , \tag{11}$$

and at $y=t$

$$A_1e^{q_1t}+A_2e^{q_2t}=B_1e^{kt}+B_2e^{-kt}\ . \tag{12}$$

Since ρ is continuous at $y=0$ and $y=t$, the jump condition, Eq. (4) requires that DW be continuous also:

$$kA=q_1A_1+q_2A_2\ , \tag{13}$$

$$q_1A_1e^{q_1t}+q_2A_2e^{q_2t}=k(B_1e^{kt}-B_2e^{-kt})\ . \tag{14}$$

The last condition is a free boundary at $y=t+\delta t$. As discussed in Sec. II, the requirement is $DW+(k^2g/\gamma^2)W=0$, and therefore

$$\left[1+\frac{kg}{\gamma^2}\right]e^{k(t+\delta t)}B_1-\left[1-\frac{kg}{\gamma^2}\right]e^{-k(t+\delta t)}B_2=0\ . \tag{15}$$

The five equations (11)–(15) are linear in the five unknowns C, A_1, A_2, B_1, and B_2. A nontrivial solution exists if and only if

$$\det(F)=0\ , \tag{16}$$

where F is the matrix

$$F=\begin{bmatrix} 1 & 0 & 0 & -1 & -1 \\ k & 0 & 0 & -q_1 & -q_2 \\ 0 & -e^{kt} & -e^{-kt} & e^{q_1t} & e^{q_2t} \\ 0 & -ke^{kt} & ke^{-kt} & q_1e^{q_1t} & q_2e^{q_2t} \\ 0 & \left[1+\frac{kg}{\gamma^2}\right]e^{k(t+\delta t)} & -\left[1-\frac{kg}{\gamma^2}\right]e^{-k(t+\delta t)} & 0 & 0 \end{bmatrix}\ . \tag{17}$$

Equation (16) reduces to

$$(q_2-k)D(q_1)-(q_1-k)D(q_2)=0\ , \tag{18}$$

where

$$D(q)=e^{qt}\left[-\left[1+\frac{kg}{\gamma^2}\right](k+q)e^{k\delta t}+\left[1-\frac{kg}{\gamma^2}\right](k-q)e^{-k\delta t}\right]\ . \tag{19}$$

Since $q_1+q_2=-\beta$ is "known," Eq. (18) is an equation for $x\sim(q_1-q_2)$ which determines γ through Eq. (9).

The stable mode is easily found: $q_1=k$ or $q_2=k$ both solve Eq. (18) with $\gamma^2=-gk$. The associated eigenfunction is $W=\text{const}\times e^{ky}$ in the whole region $-\infty\le y\le t+\delta t$.

For the rest of the modes Eq. (18) can be written, using Eq. (9) and after some algebra,

$$\tan x=\frac{2ex}{x^2+d^2-e^2-[x^2+(e-d)^2]e^{-2k\delta t}}\ . \tag{20}$$

This is a transcendental equation which has infinitely many real roots x and one imaginary root for small values[10] of kt. Of course, each root, when substituted in Eq. (9), gives a distinct growth mode γ. The faster growing modes are associated with the smaller roots x which are found, in general, by numerical techniques.

The eigenfunctions are

$$W=(A_1+A_2)e^{-\beta y/2}\left[\cos(xy/t)+\frac{1}{x}(e+d)\sin(xy/t)\right] \tag{21}$$

in the region $0\le y\le t$. In the region $t\le y\le t+\delta t$, $W=B_1e^{ky}+B_2e^{-ky}$ where

$$B_1=-(A_1+A_2)\sin x\frac{x^2+(e-d)^2}{2ex}\exp[-(e+d+2k\delta t)] \tag{22}$$

and

$$B_2=(A_1+A_2)\sin x\frac{x^2+(e+d)^2}{2ex}\exp(e-d)\ . \tag{23}$$

The constant $A=A_1+A_2$ is an undetermined overall constant which might be used for normalization.

From Eq. (9) we conclude that $\gamma\to 0$ as $kt\to 0$ and $\gamma/\sqrt{g}\to\sqrt{\beta}$ as $kt\to\infty$, i.e., $\lambda\ll t$. In this second, short-wavelength limit the roots are located at $x=\pi,2\pi,\ldots,$ and $W\sim e^{-\beta y/2}\sin(xy/t)$ in the region $0\le y\le t$. This limit is identical with the case where the exponential density profile is between two fixed boundaries.[8] In Fig. 2, we plot $\gamma^{\max}/\sqrt{g}$ vs kt_0 for the case where 50% of the mass in the original heavy shell is spread ($\delta t=t_0/2$). $\gamma^{\max}$ is the rate of the fastest growing mode.

In the same figure we show $\gamma^{\max}/\sqrt{g}$ when all the mass is spread, i.e., $\delta t=0$. In this case Eq. (20) reduces to

$$\tan x=\frac{x}{d-e} \tag{24}$$

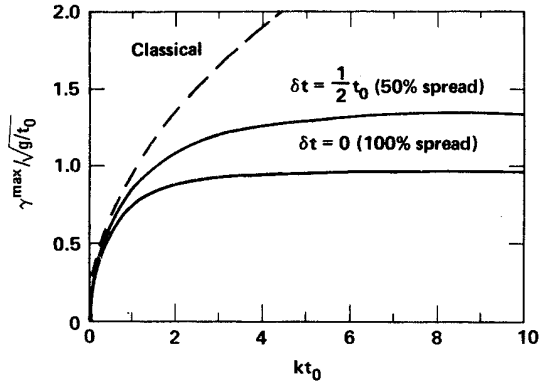

FIG. 2. Rate $\gamma^{\max}/(g/t_0)^{1/2}$ for the fastest growing mode as a function of kt_0 when 50% and 100% of the original shell is spread into an exponential profile as in Fig. 1(a) ($\delta t=\frac{1}{2}t_0$ and $\delta t=0$, respectively). The dashed curve is given by $(19kt_0/21)^{1/2}$. The continuous curves approach $\sqrt{\beta}$ where $\beta=2(1-\rho_l/\rho_h)$ and $\beta=1-\rho_l/\rho_h$ for 50% and 100% spread, respectively [Eq. (31)]. We have set $t_0=1$ for scale and $\rho_l/\rho_h=\frac{1}{20}$.

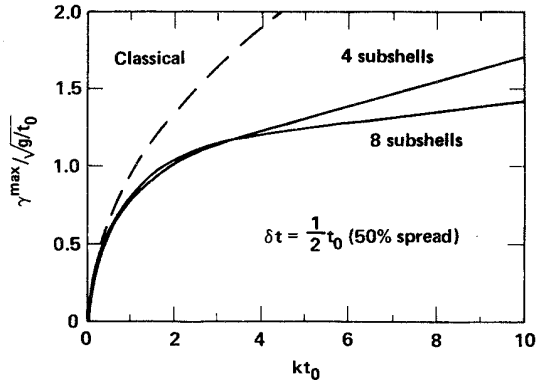

FIG. 3. Rate $\gamma^{\max}/(g/t_0)^{1/2}$ for the fastest growing mode as a function of kt_0 when 50% of the original shell is spread into four and eight subshells as in Fig. 1(b) ($\delta t=\frac{1}{2}t_0$). The dashed curve is $\sqrt{19k/21}$. The continuous curves approach $0.54\sqrt{k}$ and $0.40\sqrt{k}$ for large kt_0. We have set $t_0=1$ for scale and $\rho_l/\rho_h=\frac{1}{20}$.

while Eq. (21) remains the same (the eigenfunctions depend on δt only through x). The short-wavelength limit is again given by $\gamma/\sqrt{g}\to\sqrt{\beta}$ and $W\propto e^{-\beta y/2}\sin(xy/t)$. Since all the mass is spread, β assumes its minimum value

$$\beta_{\min}=\frac{1}{t_0}(1-\rho_l/\rho_h) \tag{25}$$

which is equal to 0.95 if $t_0=1$ and $\rho_l/\rho_h=\frac{1}{20}$.

IV. STRATIFIED DENSITY PROFILE

We would like to know how closely we can approximate the optimal exponential profile with a series of layers. Consider the case where a certain fraction of the original mass is spread into a discrete number of subshells as in Fig. 1(b). The formalism for calculating the normal modes for a stratified density profile is reported elsewhere[11] and we omit the details, giving only the results. There will be $n+2$ modes where n is the number of subshells. One of these modes is the stable mode $W\propto e^{ky}$ with $\gamma^2=-gk$ as in the preceding section. The associated growth rates γ^2 are found by solving the characteristic equation

$$\det\left|\underline{M}-\frac{gk}{\gamma^2}\underline{I}\right|=0\ , \tag{26}$$

where $\underline{M}$ is a $(n+2)\times(n+2)$ tridiagonal matrix defined by

$$M_{ij}=\begin{cases}-\rho_i/S_i(\rho_{i+1}-\rho_i), & i=j+1\\ M_{ii}, & i=j\\ -\rho_j/S_j(\rho_{i+1}-\rho_i), & i=j-1\end{cases} \tag{27}$$

otherwise $M_{ij}=0$. The diagonal elements M_{ii} are given by

$$M_{ii}=[\rho_i(T_i+1/S_i)+i\to i+1]/(\rho_{i+1}-\rho_i)\ . \tag{28}$$

In Eqs. (27) and (28) $T_i=\tanh(\frac{1}{2}kt_i)$ and $S_i=\sinh(kt_i)$, where t_i is the thickness of layer i with density ρ_i, $i=1,2,\ldots,n+2$.

For the profile shown in Fig. 1(b), $\rho_1=\rho_l$, $t_1=\infty$; $\rho_{n+2}=\rho_h$, $t_{n+2}=\delta t$, where $\delta t/t_0=1$ minus the fraction of mass spread into $\rho_2,\rho_3,\ldots,\rho_{n+1}$. We chose the thicknesses t_i of the subshells all equal to a common value $t_i=t_{\text{subshell}}$, $i=2,3,\ldots,n+1$, and the subshell densities ρ_i such that the Atwood numbers were identical at all fluid interfaces. It is easy to show that such a profile goes over to an exponential profile in the limit $n\to\infty$, and that, for finite n, $\rho_i=\rho_l(\rho_h/\rho_l)^{(i-1)/(n+1)}$, $i=1,2,\ldots,n+2$. For example, with six subshells $\rho=(1, 1.5, 2.4, 3.6, 5.5, 8.5, 13.0, 20)$ and the Atwood number at each interface is 0.21.

In Fig. 3 we plot $\gamma^{\max}/\sqrt{g}$, the rate for the fastest growing normal mode, as a function of kt_0 when half ($\delta t=t_0/2$) of the original mass is spread into four or eight subshells. Unlike the continuous case, the growth rate for the very-short-wavelength perturbations continues to increase at the rate $\gamma/\sqrt{g}\to(kN_{\text{Atwood}})^{1/2}$, where the Atwood number is 0.29 and 0.16 for four and eight subshells, respectively. Of course, $\gamma_{\text{classical}}/\sqrt{g}=(\frac{19}{21}k)^{1/2}$.

V. RESULTS AND CONCLUSIONS

Having described our method of calculation, we now turn to the results. In Fig. 4 we plot $\gamma^{\max}/\sqrt{g}$, the rate for the fastest growing mode, as a function of the fraction of the original mass $\rho_h t_0$ spread into 4, 6, 8, or ∞ (i.e., continuous) subshells. Clearly to minimize the fastest growing mode it is best to spread all of the heavy material if it can be done continuously, in which case the improvement factor $\mathscr{I}$,

$$\mathscr{I}=\gamma_{\text{classical}}/\gamma^{\max}\ , \tag{29}$$

is about 2.4. A simple discussion presented below shows that $\mathscr{I}\approx\sqrt{2\pi}$. Since in typical situations there are 8—10

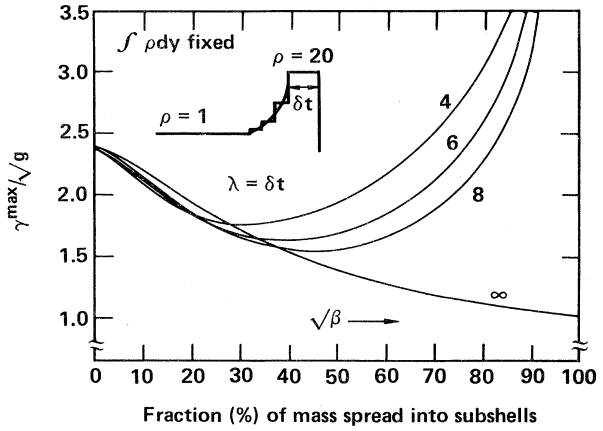

FIG. 4. Rate $\gamma^{max}/\sqrt{g}$ for the fastest growing modes as a function of the fraction of original mass spread into 4, 6, 8, and ∞ (i.e., continuous) subshells. The optimum design would spread 35%, 40%, 45%, and 100%, respectively. The total mass of the shell is kept fixed and $\lambda=\delta t=t_0(1-F)$ (F is the fraction spread). We have set $t_0=1$ for scale and $\rho_l/\rho_h=\frac{1}{20}$.

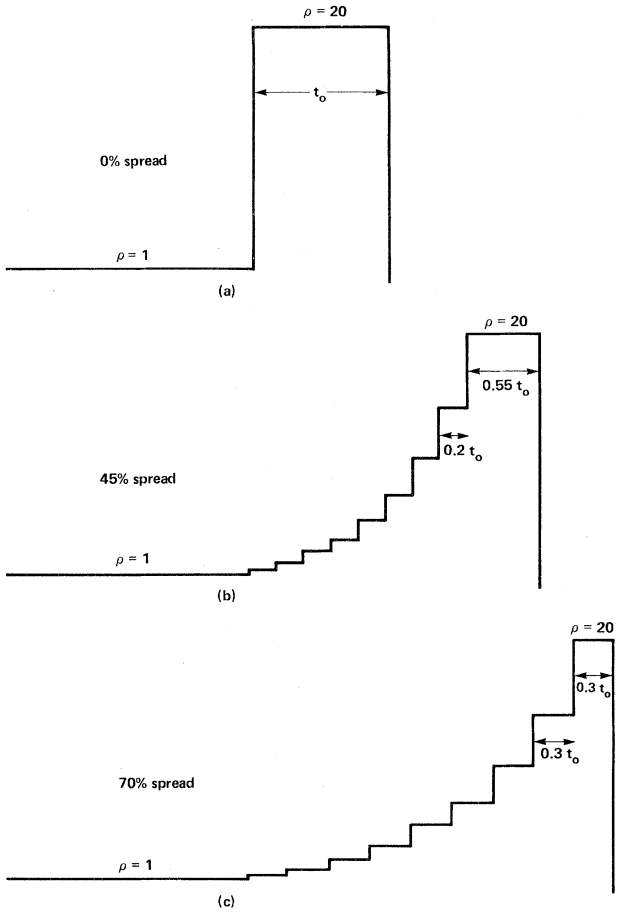

FIG. 5. (a) Original shell with no mass spread; (b) 45% mass spread into eight subshells; (c) 70% mass spread into eight subshells. For $\lambda=\delta t$, spreading 45% is best, reducing γ^{max} by a factor of 1.6. At 70% mass spread, when all the thicknesses are the same, the improvement factor is only 1.3. The density profile is (1, 1.4, 1.9, 2.7, 3.8, 5.3, 7.4, 10.3, 14.3, 20) g/cm^3.

e-foldings of growth in double-shell implosions during the shell collision, a reduction by a factor of 2.4 in the growth rate reduces the final amplitude by a factor of 100—350. This would have very important consequences for target fabrication requirements and for target performance.

In Fig. 4 conservation of mass was used to determine t: For a given fraction f of original mass spread, clearly $\delta t=(1-f)t_0=1-f$. Then we use

$$\rho_h t_0=\rho_0\delta t+\int_{\text{subshells}}\rho\, dy\ . \tag{30}$$

For n subshells, the integral becomes $t_{\text{subshells}}\sum_{i=2}^{n+1}\rho_i$, which determines $t=nt_{\text{subshells}}$. For the continuous exponential profile the integral becomes $(\rho_h-\rho_l)/\beta$, and therefore

$$\beta=\frac{1-\rho_l/\rho_h}{t_0-\delta t}\ , \tag{31}$$

which determines $t=(1/\beta)\ln(\rho_h/\rho_l)$.

As $\delta t\to 0$, the wavelength λ of the potentially dangerous perturbations also shifts to zero. These perturbations grow no faster than $\gamma^{max}/\sqrt{g}=\sqrt{\beta}$, as discussed in Sec. III. Since

$$\gamma_{\text{classical}}/\sqrt{g}=\left[\frac{2\pi(1-\rho_l/\rho_h)}{t_0(1+\rho_l/\rho_h)}\right]^{1/2}$$

for $\lambda=t_0$ in the original shell, the improvement factor is

$$\gamma_{\text{classical}}/\gamma^{max}(\delta t=0)=\left[\frac{2\pi}{1+\rho_l/\rho_h}\right]^{1/2}\approx\sqrt{2\pi}\ . \tag{32}$$

Spreading all of the mass in this manner increases the thickness of the original shell by

$$\frac{t}{t_0}=\frac{\ln(\rho_h/\rho_l)}{1-\rho_l/\rho_h} \tag{33}$$

which is about 3.

For the cases where a fraction of the heavy mass is spread into a discrete number of subshells, we note that in each case γ^{max} goes through a minimum. The existence of these minima can be understood in the following way: Spreading too little mass does not change γ much from its classical value, while spreading too much leaves such a short δt that the system becomes vulnerable to very-short-wavelength perturbations which of course grow faster when there are discrete density jumps. Somewhere in between is the best profile: For $n=4$, 6, and 8 subshells we find the best profiles if only 35%, 40%, and 45% of the heavy mass is spread, with corresponding improvement factors of 1.4, 1.5, and 1.6, respectively.

It is worthwhile to point out that the best profiles are reached *before* the thickness of each subshell matches the thickness δt of the remaining heavy shell. For example, we shown in Fig. 5 the profiles when 45% or 70% of the heavy mass is spread into eight subshells. The best profile (45% spread) of course leaves 55% in the heavy shell, hence $\delta t=0.55t_0$. We find $t_{\text{subshell}}\simeq 0.2t_0$, much thinner than δt. At 70% spread [Fig. 5(c)] $\delta t\simeq t_{\text{subshell}}=0.3t_0$, but

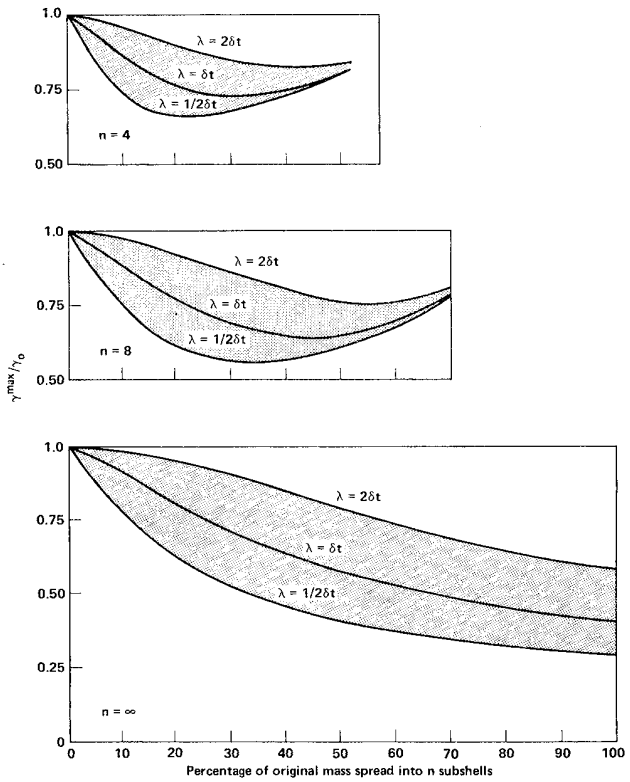

FIG. 6. Rate γ^{max} for the fastest growing modes as a function of the fraction of original mass spread into 4, 8, and ∞ subshells with three distinct choices for λ: $\lambda=\frac{1}{2}\delta t$, $\lambda=\delta t$, and $\lambda=2\delta t$. γ^{max} is normalized to γ_0, the original rate when no mass is spread.

of course by now γ^{max} is past its minimum.

As indicated in Fig. 4, we have set $\lambda=\delta t$ in each calculation of γ^{max}, and therefore λ decreases with δt as more and more of the heavy mass is spread. The choice of $\lambda=\delta t$ is motivated by the observation[12] that small perturbations grow exponentially until their amplitude becomes of order λ, after which they staturate and nonlinear effects slow down the growth. To preserve the integrity of the last shell one must guard against perturbations which might grow to the thickness δt of this shell, and hence the most dangerous wavelengths are given by $\lambda\sim\delta t$. Much shorter wavelength perturbations saturate early on, while much longer wavelenth perturbations grow too slowly. The sensitivity of our results to this assumption is shown in Fig. 6, where we plot γ^{max}/γ_0 for $n=4$, 8, and ∞ assuming, in each case, that $\lambda=\frac{1}{2}\delta t$, $\lambda=\delta t$, and $\lambda=2\delta t$. Here γ_0 is the growth rate with zero mass spread. We learn from Fig. 6 that changing λ by a factor of 2 in either direction changes the location of the minima by about 10%. Since the minima in Fig. 6 are rather broad, we conclude that stabilizing a certain design against $\lambda=\delta t$ perturbations will also reduce the growth of perturbations with $\lambda=2\delta t$ or $\lambda=\frac{1}{2}\delta t$.

We now discuss briefly the spatial structure of the eigenmodes which controls how much of the perturbation from one interface feeds through to other interfaces. In general, longer-wavelength perturbations extend further than short-wavelength perturbations, as discussed in Ref. 13. For the density profiles considered in this paper, the most unstable eigenmodes peak near the low-density region. Continuous density profiles have continuous eigenfunctions whose spatial derivatives are also continuous, unlike the step-density approximation whose eigenfunctions but not their derivatives are continuous. However, we find that the values of the eigenfunctions at the interfaces of the step-density profiles match closely the continuous-density eigenmodes and exhibit similar attenuation as one moves away from the peak.

In applications of these results to ICF implosion capsules, the assumption of incompressibility enters primarily in two ways. First, if $\gamma/k<v_s$ (v_s is the sound speed), then compression of a given initial density profile $\rho(0)=\rho(t=0)$ causes the perturbation $\eta(t)$ to vary as

$$\eta(t)/\eta(0)\approx\frac{\rho(0)}{\rho(t)}e^{\gamma t} \tag{34}$$

instead of simply $\eta(t)/\eta(0)=e^{\gamma t}$, i.e., the perturbations are compressed or expanded along with the density. To see why $\gamma/k<v_s$, note that the acceleration $g\approx P/\rho\Delta R$ where P is the pressure and ΔR is the shell thickness; hence $g\approx v_s^2/\Delta R$, and $\gamma^2/k^2=\alpha g/k\approx(\alpha/k\,\Delta R)v_s^2$ $\approx(\alpha/2\pi)v_s^2<v_s^2$, where α is the effective Atwood number which is less than 1 and is $\frac{1}{4}$ if the growth rate is reduced by a factor of 2.

Second, in the collision of two shells the material comes to nearly constant pressure and temperature. Since $P\approx[(\bar{Z}+1)/\bar{A}]\rho T$, the density varies because $(\bar{Z}+1)/\bar{A}$ is different for different materials at the 200—600 ev temperatures which are typical during collision. To maintain a density profile, then it is also necessary to have $(Z+1)/A$ vary in approximately the same ratios as the initial density. Fortunately, for normal density materials this condition is reasonably well satisfied.

We expect that during shell collision the transfer of perturbations from one side of a shell to the other is also suppressed by density gradients. Since our method assumes a constant acceleration, we cannot predict the effect of an impulsive collision except note that the initial conditions on the perturbations will be set by the collision, and these perturbations will grow as the shells accelerate.

The following example illustrates how an improvement factor of 2 in the growth rate during the acceleration phase can make a substantial difference. Assuming an aspect ratio $R/\Delta R$ of about 8 and no improvement factor one finds that initial amplitudes grow by about ten e-foldings:

$$\eta_{\text{final}}=\eta(0)e^{\gamma t},$$

$$(\gamma t)^2\approx\frac{2\pi}{\lambda}gt^2\approx\frac{4\pi}{\Delta R}R\approx 100,$$

hence $\eta_{\text{final}}=e^{10}\eta(0)$. If we require final amplitudes to be no larger than 10 μm, then initial surface finish must be about 5 Å. However, if we can achieve an improvement factor of 2 then perturbations will grow only by five e-foldings, in which case initial amplitudes of about 700 Å

can be tolerated.

Finally, we note that a useful comparison of our analytic results with those obtained from a full simulation is not quite possible at this stage because our analytic work assumes no heat transfer while numerical simulations have concentrated on ablating surfaces in which heat transfer is of course crucial. A number of simulations[4,5] have reported reduced growth rates, but it is not clear whether the reduction is due to density gradients or to heat transfer, or to both effects.

ACKNOWLEDGMENTS

We have benefited much from discussions with Dave Munro. A discussion with Chuck Hendricks on the possibilities for target fabrication was also helpful. This work was performed under the auspices of the U. S. Department of Energy by the Lawrence Livermore National Laboratory under Contract No. W-7405-ENG-48.

[1]J. Nuckolls, L. Wood, A. Thiessen, and G. Zimmerman, Nature 239, 139 (1972).

[2]J. D. Lindl and W. C. Mead, Phys. Rev. Lett. 34, 1273 (1975); J. Nuckolls, J. Lindl, W. Mead, A. Thiessen, L. Wood, and G. Zimmerman, University of California Report No. UCRL-75538, 1974 (unpublished).

[3]S. E. Bodner, Phys. Rev. Lett. 33, 761 (1974).

[4]R. L. McCrory, L. Mortierth, R. L. Morse, and C. P. Verdon, Phys. Rev. Lett. 46, 336 (1981); C. P. Verdon, R. L. McCrory, R. L. Morse, G. R. Baker, D. I. Meiron, and S. A. Orszag, Phys. Fluids 25, 1653 (1982).

[5]M. H. Emery, J. H. Gardner, and J. P. Boris, Phys. Rev. Lett. 48, 677 (1982); R. G. Evans, A. J. Bennett, and G. J. Pert, *ibid.* 49, 1639 (1982).

[6]J. D. Lindl, R. O. Bangerter, J. H. Nuckolls, W. C. Mead, and J. J. Thomson, University of California Report No. UCRL-78470, 1976 (unpublished).

[7]R. LeLevier, G. J. Lasher, and F. Bjorklund, University of California Report No. UCRL-4459, 1955 (unpublished).

[8]S. Chandrasekhar, *Hydrodynamic and Hydromagnetic Stability* (Oxford University Press, London, 1968).

[9]D. Munro (private communication).

[10]There is an imaginary root $x=iz$, z real, only if $kt<[-1+da+(1-2da+d^2)^{1/2}]/(1+a)$, where $a=e^{-2k\delta t}$.

[11]K. O. Mikaelian, Phy. Rev. Lett. 48, 1365 (1982); Phys. Rev. A 26, 2140 (1982).

[12]See, e.g., J. R. Freeman, M. J. Clauser, and S. L. Thompson, Nucl. Fusion 17, 223 (1977). B. R. Suydam, Los Alamos Informal Report LA-7291-MS, 1978 (unpublished).

[13]K. O. Mikaelian, Phys. Rev. A 28, 1637 (1983).